Unmanned aerial vehicles (UAVs) have shown promise in recent years for autonomous sensing. UAVs systems have been proposed for a wide range of applications such as mapping, surveillance, search, and tracking operations. The recent availability of low-cost UAVs suggests the use of teams of vehicles to perform sensing tasks. To leverage the capabilities of a team of vehicles, efficient methods of decentralized sensing and cooperative path planning are necessary.

The goal of this work is to examine practical control strategies for a team of fixed-wing vehicles performing cooperative sensing. We seek to develop decentralized, autonomous control strategies that can account for a wide variety of sensing missions. Sensing goals are posed from an information theoretic standpoint to design strategies that explicitly minimize uncertainty. This work proposes a tightly coupled approach, in which sensor models and estimation objectives are used online for path planning.

The experimental goal of this work is the use of a team of unmanned vehicles to search for and localize a stationary target. The vision-based sensing system used in this work is discussed in [1] and [2]. This system is unique in that it allows for target search and localization in the same software framework. Camera frames are processed to form likelihood functions, which may then be combined, in a Bayesian framework, with prior distribution to form an estimate of the target position. In this manner, the target may be localized in world coordinates. Likelihood functions may be passed between vehicles to perform search for a target cooperatively.

© U.S. AIR FORCE PHOTO/MASTER SGT. ROBERT W. VALENCA

Digital Object Identifier 10.1109/MRA.2009.932529

Autonomous UAV Path Planning and Estimation

An Online Path Planning Framework for Cooperative Search and Localization

BY JOHN TISDALE, ZUWHAN KIM, AND J. KARL HEDRICK

1070-9932/09/$25.00©2009 IEEE

Path Planning

Path planning is accomplished in a receding-horizon framework; an objective function that captures information gain is optimized at each time step, over some planning horizon. Cooperative planning is accomplished by exchanging predicted sensing actions between vehicles. To account for a limited sensor footprint, a variable planning horizon is used [3], [4].

Various approaches for searching and tracking targets using UAVs have been proposed in [5] and [6]. The development of a unified framework for search and track was proposed by Bourgault et al. [7]. Bourgault uses a grid-based probability density function (PDF) to represent target position in the plane; the precision of the estimate is limited by the resolution of the grid, and states with more than two dimensions (such as position and velocity in two dimensions) are difficult to model. For search problems with stationary targets, this approach is effective.

Previous research involving experimental mobile sensing includes work by Grocholsky [8], Cole [9], and Ross [10]. Cole et al. implemented a framework for multitarget localization using multiple UAVs. Extended Kalman filters were used for maintaining the target distributions, and a cooperative task allocation framework was used for vehicle routing. Grocholsky implemented a receding-horizon path planning framework for cooperation between UAVs and unmanned ground vehicles (UGVs); however, a coordinated approach was used, in which no planning information was shared. Information gain was predicted only for a single planning step. Ross et al. developed a system for a single vehicle to localize a stationary target using vision. A receding-horizon control approach was developed to point the camera at the target, while a Kalman filter was used for estimation. In all three cases, static targets were localized.

The work presented here is unique in that the full sensor model is incorporated explicitly into the control algorithm. Thus, an agent may evaluate the effect of an action on information gain. This work also implements an online, continuous optimization to choose a path, rather than relying on task allocation. Rather than considering some abstract utility for planning, predicted measurements from a candidate path are explicitly evaluated with respect to information gain. A fully cooperative approach is taken, in which both sensing information and future actions are shared. Lastly, the planning horizon for this optimization is allowed to vary online. By allowing a variable horizon, a more robust system is developed that can handle a variety of missions using range-limited sensors. The framework has been tested experimentally for both search and localization missions.

Sensing

A vision-based system, incorporating downward-looking cameras and onboard data processing, is used for sensing. The sensing system is explained in detail in an article by Kim [2]. In previous flight experiments, the sensing system was shown to be effective for search and localization of stationary targets. Image data is processed online to form likelihood functions that indicate the probability of an image, given the true target position. The camera was modeled as a standard pinhole camera, with uncertainty in the position, altitude, and attitude of the aircraft. The probability of target detection is dependent on the resolution, which is defined as the length compression function or the size of the target projection on the image plane. The camera coordinate system is shown in Figure 1(a).

$\mathbf{T}$ and $\mathbf{R}(\psi, \theta, \phi)$ are the position and attitude parameters of the camera. $\mathbf{Z}$ is a random variable indicating target detection. Given a detection event, $\mathbf{Z} = D$, $\mathbf{U}_T$ are the image coordinates of the target in the image. The detection likelihood (1) specifies the probability of detecting the target at image coordinates $\mathbf{U}_T$, given that the target is at world coordinates $\mathbf{X}$ and given aircraft position and attitude estimates $\widehat{\mathbf{T}}, \widehat{\mathbf{R}}$.

$$P(\mathbf{U}_T, \mathbf{Z} = D | \mathbf{X}, \widehat{\mathbf{T}}, \widehat{\mathbf{R}}). \tag{1}$$

The likelihood in (1) accounts for localization. Uncertainty in position and attitude estimates is incorporated into the likelihood function by convolving probability distributions for these estimates with a Taylor series approximation of the transformation from world to image coordinates.

$$P(\mathbf{U}_T | \mathbf{X}, \widehat{\mathbf{T}}, \widehat{\mathbf{R}}) = \int_{\mathbf{R}} \int_{\mathbf{T}} P(\mathbf{U}_T | \mathbf{X}, \mathbf{T}, \mathbf{R}) P(\widehat{\mathbf{R}} | \mathbf{R}) P(\widehat{\mathbf{T}} | \mathbf{T}) d\mathbf{T} d\mathbf{R}. \tag{2}$$

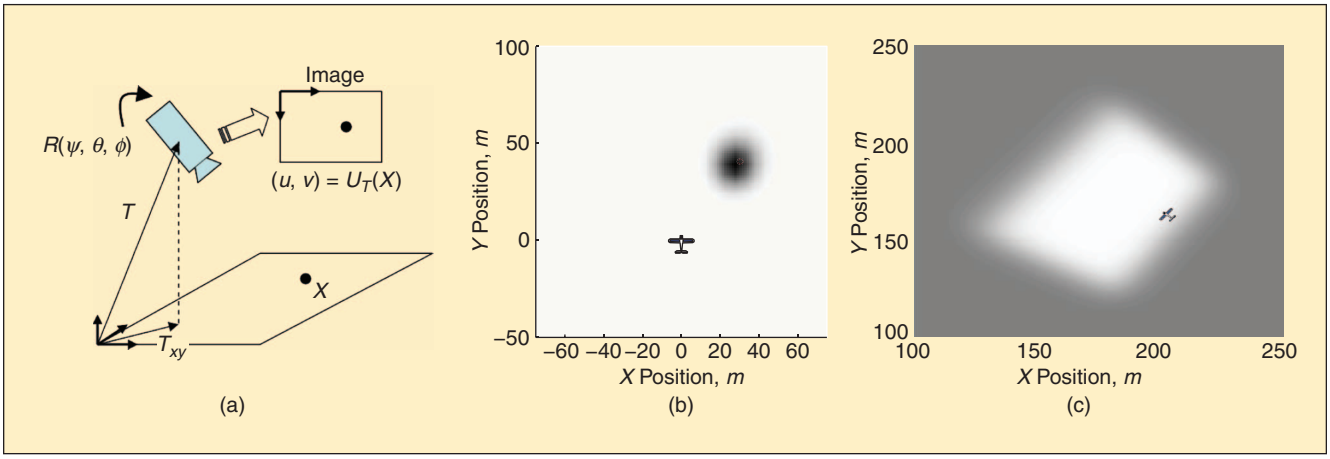

Figure 1. *Camera coordinates and example likelihood functions. (a) Camera coordinates. (b) Detection likelihood function. (c) No detection likelihood function.*

Here, (3) gives the probability of not detecting a target in the image frame, given that the target is at some world coordinates $\mathbf{X}$. This likelihood function indicates which points do not contain the target and accounts for target search.

$$P(\mathbf{Z} = -D|\mathbf{X}, \widehat{\mathbf{T}}, \widehat{\mathbf{R}}). \tag{3}$$

These likelihood functions may be combined, using various Bayesian filtering techniques, to find the distribution of the target position [1].

Figure 1 indicates sample detection and no detection likelihood functions. Light areas indicate values close to zero, and darker areas indicate values closer to one.

Filtering

A recursive Bayesian framework is used to fuse likelihood functions to form a probability distribution representing target position. Both the detection and no detection likelihood functions are nonlinear and non-Gaussian, which precludes many filtering schemes, such as the Kalman filter. Because of these nonlinearities, a grid-based scheme is used to maintain the distribution.

Recursive Bayesian estimation is a general framework for applying sensor data and a target model to a prior probability distribution to form an estimate. Bayesian estimation consists of a prediction step and an update step. In this case, the sensor model is represented by the likelihood function $P(\mathbf{Z}_k|\mathbf{X}_k)$, where k represents the time step. The target is represented by a process model $P(\mathbf{X}_{k+1}|\mathbf{X}_k)$. In the update state (4a), sensor data $\mathbf{Z}_k$ is applied. In the prediction step (4b), the process model is used to estimate the distribution at time $k+1$, based on the distribution at time k.

$$P(\mathbf{X}_k|\mathbf{Z}_{1:k}) = \frac{P(\mathbf{Z}_k|\mathbf{X}_k)P(\mathbf{X}_k|\mathbf{Z}_{1:k-1})}{P(\mathbf{Z}_k|\mathbf{Z}_{1:k-1})}. \tag{4a}$$

$$P(\mathbf{X}_{k+1}|\mathbf{Z}_{1:k}) = \int P(\mathbf{X}_{k+1}|\mathbf{X}_k)P(\mathbf{X}_k|\mathbf{Z}_{1:k})d\mathbf{X}_k. \tag{4b}$$

Targets in the work are assumed to be stationary. Thus, the filtering system is simplified, as a prediction step is unnecessary. A detailed discussion of this filtering system, and other approaches, is discussed in [1]. For the sake of cooperation, exactly parameterized likelihood functions were passed between vehicles over an ad hoc network. This approach allows for a global estimate of the target to be maintained on all vehicles.

Path Planning

The goal of the control scheme is to maximize an objective function representing information gain.

$$\mathbf{U}^* = \arg\max_{\mathbf{U}} J(\mathbf{U}), \tag{5}$$

where $\mathbf{U} = \{U_1, \ldots, U_K\}$ are the control inputs over K time steps, subject to some constraints, and $J(\mathbf{U})$ is a reward function that captures the value of the information collected. For a general sensing problem, computing the optimal control sequence $\mathbf{U}^*$ is intractable for any significant problem length. To make the problem tractable, a receding-horizon approach is used, where optimal solutions are computed for a short time horizon, N, at a fixed interval.

$$\mathbf{U}^*_{k:N+k} = \arg\max_{U_{k:N+k}} J(\mathbf{U}_{k:N+k}|\mathbf{U}_{1:k-1}). \tag{6}$$

In this work, a gradient-based approach is used to solve for optimal paths. The actual objective function used in this work is introduced later in this section. Generally, this optimization is nonconvex, and convergence to a local minimum is all that may be guaranteed. The use of multiple initial conditions may decrease the chance of selecting a nonglobal minimum. Given that this optimization problem must be solved online, the use of computationally efficient structures is necessary.

Long-Term Planning

Many receding-horizon strategies use a terminal cost to account for long-term goals. The use of a terminal cost allows for effective paths to be planned in a myopic situation when there is no information to be gained within the planning horizon. In this work, a different approach is used to deal with myopia. The goal of this scheme is to choose a planning horizon to ensure that every plan has a value above some threshold.

When $J(\mathbf{U}^*_{k:N+k})$ is less than some threshold, ε, the planning horizon is increased; however, as the planning horizon is increased, a different optimization strategy is employed. This strategy is referred to as an *increasing horizon planner*, shown in Algorithm 1. Given some planning horizon, k_h, the planner selects the best possible measurement within the vehicle reach set, `Reach`(k_h). If the value of that measurement is above some threshold ε, a path is planned to make that measurement; if the value is not large enough, the horizon is increased, and another plan is made. This approach decreases the dimensionality of the optimization at each iteration.

For a threshold ε, plans will be within $(k_h - 1)\varepsilon$ of the maximum value obtained by the optimal path, as all previous measurements for $k < k_h$ have value less than ε. For the search problem detailed here, this planner can be run efficiently when

Algorithm 1: Increasing Horizon Planner

1) **while** $J(\overline{\mathbf{Z}}_{k:k_h}) <$ *threshold* **do**
2) $\overline{\mathbf{Z}}_{k_h} = \arg\max_{\mathbf{Z} \in Reach(k_h)} J(\mathbf{Z}_{k_h})$
3) $k_h = k_h + 1$
4) Calculate shortest path, $\mathbf{Y}_{1:k_h}$ to take measurement $\overline{\mathbf{Z}}_{k_h}$
5) Find measurement sequence $\overline{\mathbf{Z}}_{k:k_h-1}$ for path $\mathbf{Y}_{1:k_h}$
6) **end while**

The recent availability of low-cost UAVs suggests the use of teams of vehicles to perform sensing tasks.

the modes of the PDF, within the reachable set, may be evaluated quickly, to seed the unconstrained optimization (Algorithm 1, line 2). When the probability distribution is stored as a grid, evaluation of the modes is computationally efficient. For other representations, such as a particle filter, a different approach might be necessary. Also, the shortest path must easily be calculated. For a UAV with a constrained turn-rate, Dubin's paths are the optimal trajectories between any two points and are quickly calculated [11].

In this work, a simplified reach set was used. Attitude angles were not used in the optimization. For computational efficiency, a circular approximation of the reach set was used for planning steps with large k_h. In future work, this procedure could be refined by optimizing over the exact reach set.

Information Measures

For the sake of search and localization, appropriate objective functions include probability of detection (POD) and entropy. The entropy of a probability distribution $\mathcal{H}(P(\mathbf{X}))$ is a measure of uncertainty. For a continuous distribution,

$$\mathcal{H}(P(\mathbf{X})) = -\int P(\mathbf{X})\log(P(\mathbf{X}))d\mathbf{X}. \tag{7}$$

The reduction in entropy due to conditioning on a series of future measurements $\mathbf{Z}$ is referred to the mutual information (MI):

$$\mathrm{MI}(\mathbf{X};\mathbf{Z}) = \mathcal{H}(P(\mathbf{X})) - \mathcal{H}(P(\mathbf{X}|\mathbf{Z})), \tag{8}$$

$$\mathcal{H}(P(\mathbf{X}|\mathbf{Z})) = \mathop{\mathbf{E}}_{\mathbf{X},\mathbf{Z}}\left[-\log\frac{P(\mathbf{X}|\mathbf{Z})}{P(\mathbf{X})}\right]. \tag{9}$$

MI is a measure of the information about $\mathbf{X}$ contained in $\mathbf{Z}$. In evaluating a trajectory for sensing, MI is an intuitive measure of the value of a series of measurements, prior to taking those measurements. With respect to a search problem, entropy minimization can be thought of as localization, not necessarily requiring that the target be detected. This measure is used in many sensing problems [9].

Given $P(\mathbf{X})$, and a series of future observations $\mathbf{Z}_{1:k}$ that are a function of the vehicle path, the probability of detecting the target in each of those observations may be calculated. This gives rise to the cumulative POD or the probability that the target will be detected, at least once, over some series of observations. Define Q as the probability of not detecting a target, for sensor readings 1 to k for m vehicles

$$Q(\mathbf{Z}_{1:k}^{1:m}) = \int P(\mathbf{X})\prod_{i=1}^{m}\prod_{j=1}^{k} P(\mathbf{Z}_j^i = \bar{D}|\mathbf{X};\mathbf{Y}_j^i)d\mathbf{X}. \tag{10}$$

Then, the cumulative POD at time k is equal to $1 - Q(\mathbf{Z}_{1:k}^{1:m})$ [12].

Generally, computing an information measure for a distribution is computationally expensive. To compute MI, an expectation must be taken over both target state $\mathbf{X}$ and observations $\mathbf{Z}$. For the sake of computing the POD, this problem becomes quite easy. While MI is in many ways a more general objective function, POD was used in this work due to the ease of computation. This function was used as the objective for the optimization in (6), by considering that the measurements $\mathbf{Z}$ are a function of the vehicle path, and thus the control $\mathbf{U}$. For POD, it is assumed that the target is not detected at each time step, and thus no integration over observations is necessary. Only an integration over the target state is necessary; this computation is simply a two-dimensional integral and may be calculated quickly in the control loop. By comparison, computation of MI would be a four-dimensional integral, over both sensor values and target state.

In this work, the relationship between the control $\mathbf{U}$ and the vehicle state $\mathbf{Y}$ is assumed to be deterministic. Clearly, this is not the case, as no controller will produce a perfect path. However, taking an expectation over vehicle paths is computationally expensive and quite likely would not produce any real performance gain.

Cooperation

In this work, we consider teams of vehicles, cooperating to maximize the same objective function. Rather than consider (6) which represents a reward function for a single vehicle, we consider (11) to account for the decisions of multiple vehicles.

$$\mathbf{U}^* = \arg\max_{\mathbf{U}} J(U_{1:k}^1, \ldots, U_{1:k}^m), \tag{11}$$

where $\mathbf{U} = \{U_{1:k}^1, \ldots, U_{1:k}^m\}$ are the control inputs of the m team-members over k time steps, subject to some constraints. There is a significant amount of research on solving optimization problems cooperatively [13]. Although these procedures will yield a (locally) optimal solution, these schemes are generally too computationally expensive to implement on a real-time system.

Rather than implement a team-optimal solution, a greedy policy is used. Controls chosen by a greedy policy $\widehat{\mathbf{U}}$ are defined by

$$\widehat{\mathbf{U}}^i = \arg\max J(\mathbf{U}^i|\widehat{\mathbf{U}}^1, \ldots, \widehat{\mathbf{U}}^{i-1}). \tag{12}$$

A greedy policy is one in which measurements are selected sequentially to optimize the cost function, based on all previously selected measurements; i.e., $\widehat{\mathbf{U}}^1 = \arg\max J(\mathbf{U}^1)$ and $\widehat{\mathbf{U}}^2 = \mathrm{argmax}\, J(\mathbf{U}^2|\widehat{\mathbf{U}}^1)$. Conditioning is defined by

$$J(\mathbf{U}^1|\mathbf{U}^2) = J(\mathbf{U}^1, \mathbf{U}^2) - J(\mathbf{U}^2). \tag{13}$$

For submodular and nondecreasing objective functions, a lower bound on the optimality of the greedy policy may be established.

Definition 1 (Submodular): A set function f is submodular if $f(C \cup A) - f(A) \geq f(C \cup B) - f(B)\ \forall\ A \subseteq B$. Submodularity captures the notion that the more measurements one adds to a pool, the less valuable an individual measurement becomes

$$J(Z^1, Z^2) - J(Z^2) \geq J(Z^1, Z^2, Z^3) - J(Z^2, Z^3).$$

One consequence of submodularity is that $J(Z^2) \geq J(Z^2|Z^1)$.

Definition 2 (Nondecreasing): A set function f is nondecreasing if $f(B) \geq f(A)\ \forall\ A \subseteq B$. The nondecreasing property implies that the addition of a measurement always increases your reward,

$J(Z^1, Z^2) \geq J(Z^1)$; taking into account the observation of a target, on average, cannot increase your uncertainty.

Given a submodular, nondecreasing objective function, a greedy policy yields plans that are, at worst, half the value of the optimal solution, regardless of the number of agents [14]. Specifically, the greedy algorithm yields a policy, where

$$J(\mathbf{U}^*) \leq 2J(\widehat{\mathbf{U}}). \tag{14}$$

Both MI and POD are submodular and nondecreasing [3]. The full-planning algorithm is shown in Algorithm 2. A greedy algorithm is used for cooperation, while a variable horizon is used when vehicles are not in an area of local value. It is important to note that this algorithm allows each vehicle to plan to a different horizon when necessary. The bound of (14) applies when vehicles are planning to the same horizon.

Algorithm 2: Planning Algorithm for *i*th Vehicle

1) Receive predicted measurements, $\mathbf{Z}_{k:k_h}^{1:i-1}$, from other vehicles
2) Apply predicted measurements to distribution $P(\overline{\mathbf{X}}_{k_h}) = P(\mathbf{X}_k)P(\mathbf{Z}_{k:k_h}^{1:i-1} = \bar{D}|\mathbf{X})$, assuming no-detect
3) $\widehat{\mathbf{U}} = \arg\max_{\mathbf{U}} J(\mathbf{U}, P(\overline{\mathbf{X}}_{k_h}))$
4) If $J(\widehat{\mathbf{U}}) < \varepsilon$ execute Algorithm 1 (Increasing Horizon Planner).
5) Calculate path, $\mathbf{Y}$, based on $\widehat{\mathbf{U}}$
6) Calculate predicted measurements, $\mathbf{Z}_{k:k_h}^{i}$ based on path $\mathbf{Y}$.
7) Transmit measurement sequence $\mathbf{Z}_{k:k_h}^{i}$

Experimental Setup

The Berkeley UAV platform is based on a Sig Rascal airframe shown in Figure 2. This airframe has a 110-in wing span and carries 14 lb of payload at a gross weight of 27 lb. Cruise speed for the platform is 20 m/s. A Piccolo global positioning system (GPS) and pitot-static avionics package, produced by Cloudcap Technologies, is used for low-level aircraft control. Various cameras are available for flight experiments. In this work, fixed, downward-looking bullet cameras, with resolution of 240 × 320 pixels, were used. An onboard 1.8-GHz Pentium PC104 system performs high-level planning, video processing, and control. An 802.11b ad hoc network allows for intervehicle and ground communication. The user may guide the vehicles in their search by entering probability distributions using a graphical interface. For further information, see [15].

To solve the optimization problem in (6), a gradient-based solver was used to find solutions in fixed time. Although various software packages were evaluated to solve this problem, a simple gradient-based solver was developed to guarantee fixed-time computation and to allow for application-specific modification. The solver was seeded with a variety of initial conditions, at each time step, to reduce the chance of converging to a nonglobal minimum. A separate low-level tracking controller was employed for flying the path developed by the path planner. The tracking controller is based on a spatial sliding mode controller [16]. The control schematic may be seen in Figure 2.

For receding-horizon path planning, a unicycle model of the aircraft was used, discretized at 1-s intervals. Actual sensing occurred at roughly 4 Hz. The initial horizon for the path planner was set to 8–15 s with replanning occurring every 1–3 s. An extended Kalman filter was used to filter GPS and attitude data, as the Piccolo avionics system delivers GPS updates at only 4 Hz. Missions were flown at 80 and 110 m to prevent possible collisions between aircrafts. A square grid of 6,400 cells was used to model the probability distribution over 1 km^2. The targets used were 3-m red tarps.

Hardware-in-the-Loop Simulation Results

Prior to flight test, the system was tested on a six degrees of freedom (DoF) hardware-in-the-loop setup, with flight avionics and software. The first example, in Figure 3(a) and (b), illustrates the value of long-term cooperative planning. A prior target distribution was specified over four small, geographically distinct areas, at each corner of a 1-km square box. Dark areas indicate high probability of target, while light areas indicate low probability. Black dots indicated desired vehicle path. Each vehicle began the simulation far from the areas of interest and thus made long-term plans. Initially, each vehicle was closest to the point at (0,0). By exchanging predicted likelihoods

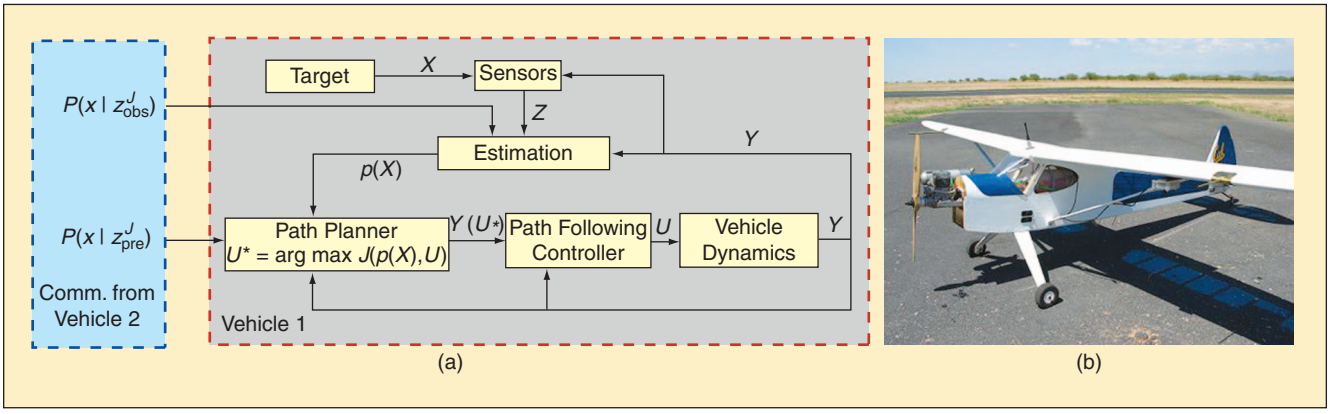

Figure 2. *(a) Control and sensing architecture and (b) the flight platform at the University of California, Berkeley.*

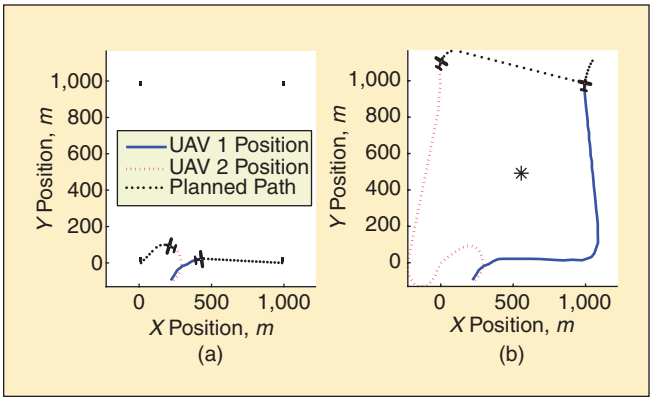

Figure 3. *Vehicle trajectory and target distribution at various times for hardware-in-the-loop simulation: (a) $t = 5$ and (b) $t = 68$.*

functions, a plan was formed that takes only one vehicle to each target. Far from the target, long plans were made using Algorithm 1. As each vehicle approached an area of significant probability, short-term plans were made, using the gradient-based planner. This example illustrates the value of an adjustable planning horizon.

The system was also tested to examine the effects of short-term cooperation. Figure 4 shows trajectories for a pair of vehicles searching for a target. The simulation was run cooperatively and without cooperation (coordinated). In the coordinated simulation, vehicles only exchanged likelihood functions or observed information. They exchanged no information regarding future plans. For 100 s of searching, the cooperative solution yields a POD of 90%, compared to 66% in the noncooperative case.

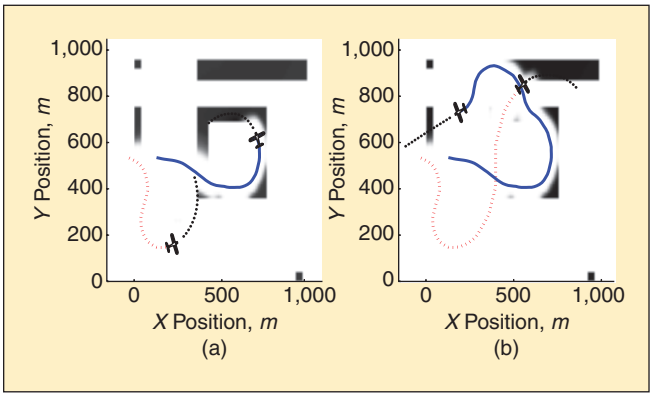

Figure 4. *Vehicle trajectory and target distribution at various times for hardware-in-the-loop simulation: (a) $t = 37$ and (b) $t = 91$.*

Experimental Results

Flight experiments were performed at Camp Roberts, California, in January 2008. A series of missions were flown to search for and localize a target. Initially, a single plane was used; cooperative flights with two aircrafts were also flown. Experiments were performed with and without targets to evaluate both search and localization performance.

The aircraft was tasked to localize a target with a prior probability distribution contained within a small area, shown in Figure 5(a). For this flight, a 15-s planning horizon was specified, discretized at 1-s intervals. If the threshold was not reached within the initial 15-s horizon, the discretization was doubled, leading to a 30-s planning horizon. If the threshold was not reached with a 30-s planning horizon, the increasing-horizon planner is used. In this experiment, the gradient-based planning horizon was long enough to ensure that the gradient-based scheme was used almost throughout the entire experiment. The scheme switches between a discretization of 1 s, as in Figure 5(b), and 2 s, as in Figure 5(a). Examination of the final plot indicates that a clover leaf pattern emerges from this control scheme, leading to four passes where the sensor captures the target in frame. Localization error for this flight was 6.7 m.

A single plane was tasked to search for a target over the prior probability distribution shown in Figure 6(a). This distribution was uniform over portions of the runway and roads to the north and south. To force the aircraft to search the entire prior distribution, no targets were placed on the field. The wind during this flight was 8 m/s with significant gusts from the northwest.

Due to the wind, the vehicle is unable to search the northwestern portion of the road on the first pass, as seen in Figure 6(b) and must return after searching the southern road in Figure 6(c). Plots of POD and entropy are shown in Figure 6(d). The prior was searched at a rate of 0.0049 units probability mass per second. The use of a gradient-based planning scheme, which accounts for the full sensor model, allows the vehicle to fly a path that captures this oddly shaped prior distribution.

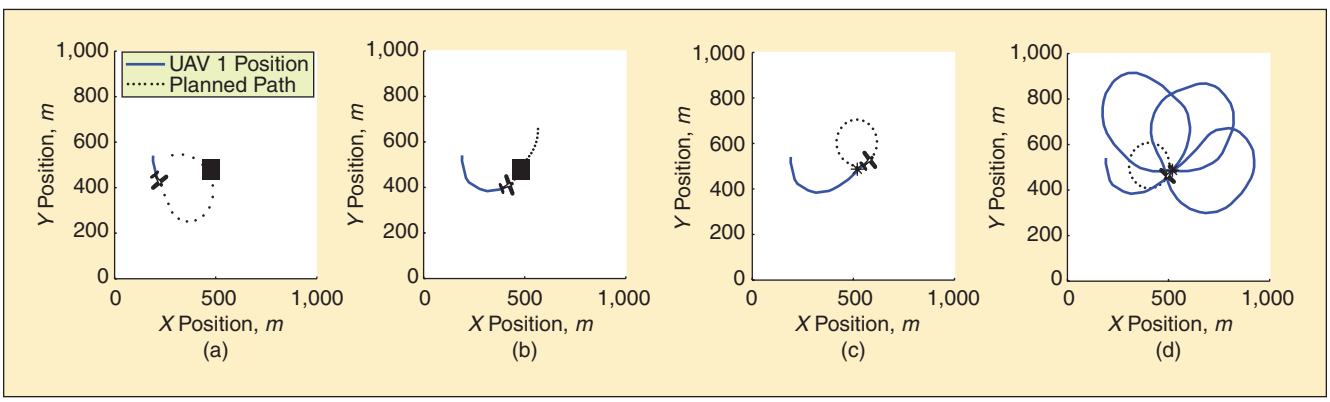

Figure 5. *Vehicle trajectory and target distribution at various times for localization flight: (a) $t = 4$, (b) $t = 10$, (c) $t = 16$, and (d) $t = 112$.*

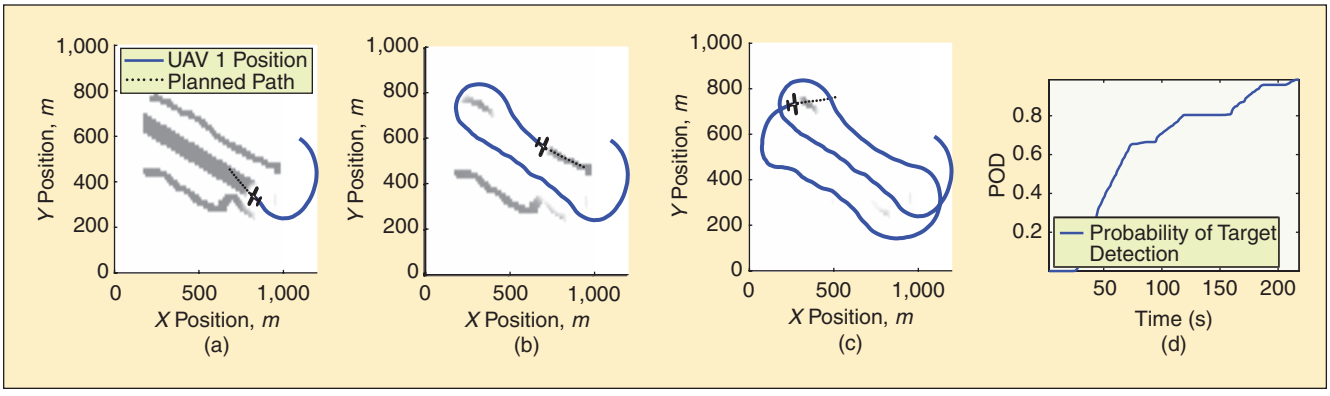

Figure 6. *Vehicle trajectory and target distribution at various times for search flight: (a) $t = 35$, (b) $t = 107$, (c) $t = 210$, and (d) POD.*

The system was also tested for cooperative search with two aircrafts. Figure 7 illustrates trajectories for the cooperative search flight. The vehicles were effective in searching the prior distribution.

For the first half of the experiment, the area was searched at a rate of 0.009 units of probability mass per second, nearly double the rate of the single plane flight. Figure 7(a) illustrates the problem of cooperative planning with different horizons. In this figure, UAV 1 is planning to search an area slightly ahead of where UAV 2 is planning to search. This poor performance is due to planning on different horizons and has been addressed in [3]. Fortunately, as the flight progresses, the vehicles plan to the same horizon and converge on a better plan, as seen in Figure 7(b).

The system was also tested for cooperative localization performance. In this case, an actual target was used. Figure 8 shows snapshots of the search and localization paths, for a pair of aircrafts. UAV 1 was the first to localize the target. UAV 2, upon receiving likelihood functions from UAV 1, plans a path to the target as well and further localizes the target. Fundamentally, search and localization are different objectives. Figure 8 indicates the effectiveness of a single framework for both objectives. Examination of an entropy plot [Figure 8(d)] indicates that the primary entropy drop comes, not surprisingly, from the initial detection of the target by UAV 1. The information gain from the second UAV, at $t = 148$, is relatively trivial, although it does contribute to better localization.

Localization error in this case was 2.9 m. The final posterior distribution contained all probability mass on one grid, indicating 3σ ellipse of 18.97 m, which is the minimum possible covariance for these grid parameters. Post-processing, with a finer grid, yielded an error of 1.5 m.

In this case, the trajectories generated for target search were not the most efficient; however, the vehicles were successful in effectively localizing the target. For this flight, a planning horizon of 8 s was used, with 3-s replanning intervals. Significantly better results might be obtained by using a longer planning horizon, such as in the single-aircraft localization example.

Conclusions

Flight experiments have demonstrated the capability for unmanned vehicles to perform autonomous search and localization in a cooperative setting, using receding-horizon path planning. This work is unique in that the effect of sensing, represented by the full sensor model, is directly incorporated into the control scheme, in a cooperative framework. The use of a variable planning horizon allows for a wide variety of missions to be performed.

Many receding-horizon strategies have been proposed that plan only a single step into the future. This work shows that, for systems with constrained sensor footprints, multistep planning is important, and in some cases necessary, for good performance. Even within this work, planning horizon issues greatly affected system performance. The use of a variable planning horizon strategy allows for this system to account for both search and localization problems.

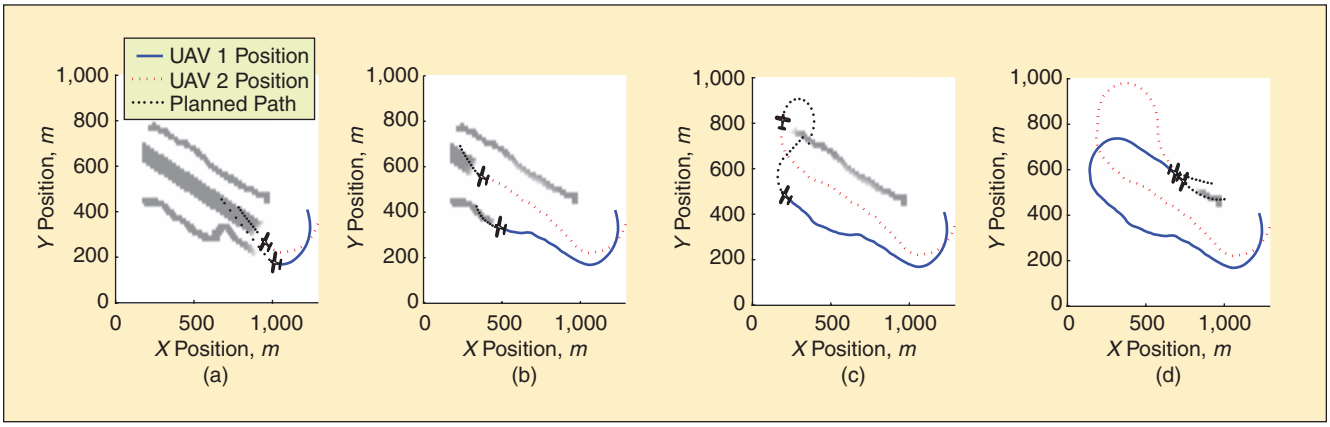

Figure 7. *Vehicle trajectories and target distribution at various times for cooperative search flight: (a) $t = 21$, (b) $t = 53$, (c) $t = 70$, and (d) $t = 105$.*

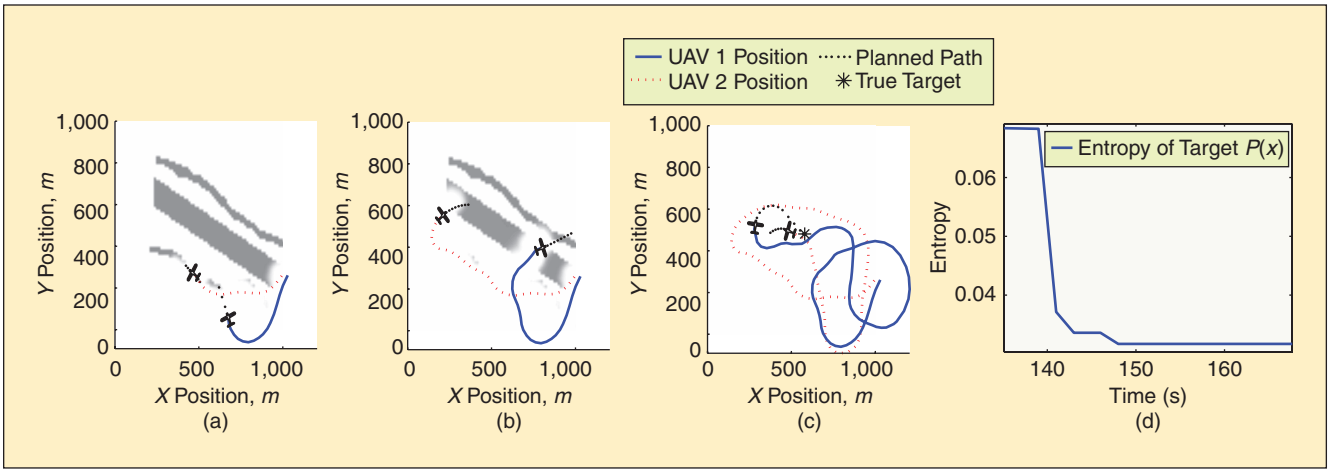

Figure 8. *Vehicle trajectories and target distribution for localization flight: (a) $t = 31$, (b) $t = 58$, (c) $t = 164$, and (d) entropy.*

By posing path planning as a trajectory optimization problem, a general control framework has been developed. It is our hope that this structure can be applied to many different types of sensing problems, such as multiple-moving target tracking, using MI as an objective function. A change in application would simply require different filtering procedures and objective functions; much of the basic structure could remain the same.

Keywords

Path planning, unmanned vehicles, information-based control.

References

[1] J. Tisdale, A. Ryan, Z. Kim, D. Tornqvist, and J. K. Hedrick, "A multiple UAV system for vision-based search and localization," in *Proc. IEEE American Controls Conf.*, 2008, pp. 1985–1990.

[2] Z. Kim and R. Sengupta, "Target detection and position likelihood using an aerial image sensor," in *Proc. IEEE Int. Conf. Robotics and Automation*, 2008, pp. 59–64.

[3] J. Tisdale, J. K. Hedrick, and H. Durrant-Whyte, "Path planning for cooperative sensing using unmanned vehicles," in *Proc. ASME Int. Mechanical Engineering Conf. Exposition*, Seattle, Washington, 2007.

[4] J. Tisdale, Z. Kim, and J. K. Hedrick, "An autonomous system for cooperative search and localization using unmanned vehicles," presented at the AIAA Guidance, Navigation and Control Conf., 2008.

[5] G. Conte, M. Hempel, P. Rudol, D. Lundstrom, S. Duranti, M. Wzorek, and P. Doherty, "High accuracy ground target geo-location using autonomous micro aerial vehicle platforms," presented at the AIAA Guidance, Navigation and Control Conf., 2008.

[6] M. E. Campbell and M. Wheeler, "A vision based geolocation tracking system for UAVs," in *Proc. AIAA Guidance, Navigation, and Control Conf. Exhibit*, Aug. 2006.

[7] T. Furukawa, F. Bourgault, B. Lavis, and H. Durrant-Whyte, "Recursive Bayesian search-and-tracking using coordinated UAVs for lost targets," in *Proc. IEEE Conf. Robotics and Automation*, Orlando, Florida, 2006.

[8] B. Grocholsky, J. Keller, V. Kumar, and G. Pappas, "Cooperative air and ground surveillance," *IEEE Robot. Automat. Mag.*, vol. 13, no. 3, pp. 16–25, Sept. 2006.

[9] D. T. Cole, A. H. Goktogan, and S. Sukkarieh, "The demonstration of a cooperative control architecture for UAV teams," in *Proc. 10th Int. Symp. Experimental Robotics*, Rio de Janeiro, Brazil, 2006, pp. 501–510.

[10] J. A. Ross, B. R. Geiger, G. L. Sinsley, J. F. Horn, L. N. Long, and A. F. Niessner, "Vision-based target geolocation and optimal surveillance on an unmanned aerial vehicle," presented at the AIAA Guidance, Navigation and Control Conf., 2008.

[11] L. E. Dubins, "On curves of minimal length with a constraint on average curvature and with prescribed initial and terminal positions and tangents," *Am. J. Math.*, vol. 79, no. 3, pp. 497–516, 1976.

[12] F. Bourgault, T. Furukawa, and H. Durrant-Whyte, "Optimal search for a lost target in a Bayesian world," in *Proc. Int. Conf. Field and Service Robotics*, 2003, pp. 209–222.

[13] G. Mathews, H. Durrant-Whyte, F. Bourgault, and T. Furukawa, "Decentralised asynchronous optimisation and team decision making," in *Proc. IEEE Conf. Decision and Control*, Atlanta, 2007.

[14] J. Williams, "Information theoretic sensor management," Ph.D. dissertation, Department of Electrical Engineering and Computer Science, Massachusetts Institute of Technology, 2007.

[15] J. Tisdale, A. Ryan, M. Zennaro, X. Xiao, D. Caveney, S. Rathinam, J. K. Hedrick, and R. Sengupta, "The software architecture of the Berkeley UAV platform," in *Proc. IEEE Conf. Control Applications*, 2006, pp. 1420–1425.

[16] S. Jackson, J. Tisdale, M. Kamgarpour, B. Basso, and J. K. Hedrick, "Tracking controllers for small UAVs with wind disturbances: Theory and flight results," in *Proc. IEEE Conf. Decision and Control*, Dec. 2008, pp. 564–569.

John Tisdale obtained his B.Sc. degree in aerospace engineering from the University of Texas, Austin, and his Ph.D. degree in mechanical engineering at the University of California, Berkeley, in 2008. Currently, he is a research scientist at 510 Systems, Berkeley, California. His primary interests are unmanned vehicle control, navigation, and estimation.

ZuWhan Kim obtained his Ph.D. degree in computer science from the University of Southern California, in 2001. He is a researcher with the Institute of Transportation Studies, University of California, Berkeley, California. His primary research areas are computer vision, pattern recognition, and machine learning. He is a Member of the IEEE.

J. Karl Hedrick is the James Marshall Wells professor of mechanical engineering at the University of California at Berkeley, where he teaches graduate and undergraduate courses in automatic control theory. He is currently the director of Berkeley's Vehicle Dynamics Laboratory as well as the principal investigator of the Center for the Collaborative Control of Unmanned Vehicles.

Address for Correspondence: John Tisdale, 2101 Dwight Way, Suite 2070, Berkeley, CA 94704, USA. E-mail: jtisdale@berkeley.edu.